



Assessing the Environmental Situation of Euphrates River Sediments Using Magnetic Susceptibility Techniques in Al-Muthanna Province, Southwestern Iraq

Nawrass N. Ameen^{1*} 

¹ college of science, University of Al Muthanna, Al Muthanna, Iraq.

Article information

Received: 27- Aug -2024

Revised: 20- Oct -2024

Accepted: 15- Jan -2025

Available online: 01- Jan – 2026

Keywords:

Sediment Contamination
Magnetic, Mineralogy,
Heavy Metals,

ABSTRACT

Sediment contamination is one of the major challenges the Euphrates River environment faces. The Euphrates River is regarded as the main supply of water for industrial and agricultural purposes for Samawa City in Al Muthanna Province, the southwestern part of Iraq. The sewage pipeline is dumped into the river, which directly affects the water quality and subsequently the vegetation. A magnetic mineralogy study is carried out on sediments to specify the contamination by heavy metals. Magnetic properties are measured in 250 sediment samples; magnetic susceptibility, anhysteretic remanent magnetization, isothermal remanent magnetization, and thermomagnetic analyses are measured. Heavy metal analyses are performed using SEM together with energy-dispersive X-ray and X-ray fluorescence analyses to connect the results with magnetic enhancements. Statistical analyses show that the mean value of magnetic susceptibility is 3361.2×10^{-8} m³kg⁻¹, of anhysteretic remanent magnetization is 628.9×10^{-8} m³kg⁻¹, and thermomagnetic analyses (high and low) clearly show the typical curves of magnetite. The magnetic properties results indicate that the main magnetic phases are single-domain (SD) to multi-domain (MD) state magnetite caused by the surrounding catchment and anthropogenic activities. Results of heavy metal (HM) analysis performed on ten selected samples and then compared with the magnetic results. A correlation between HM and χ shows a positive correlation between magnetic susceptibility and Ca, Cr, Mg, Fe, Pb, and Na concentrations. The results of magnetic mineralogy indicate that the magnetic susceptibility parameter can be used as an indicator for heavy metals.

Correspondence:

Name: Nawrass N. Ameen

Email: nawrass@mu.edu.iq

DOI: [10.33899/injes.v26i1.60182](https://doi.org/10.33899/injes.v26i1.60182), ©Authors, 2026, College of Science, University of Mosul.
This is an open-access article under the CC BY 4.0 license (<http://creativecommons.org/licenses/by/4.0/>).

تقييم الوضع البيئي لرواسب نهر الفرات باستخدام تقنيات الحساسية المغناطيسية في محافظة المثنى، جنوب غربي العراق

نورس امين^{1*} 

¹ كلية العلوم، جامعة المثنى، المثنى، العراق.

الملخص

يعد تلوث الرواسب من أهم التحديات التي تواجه بيئة نهر الفرات، حيث يعتبر نهر الفرات المصدر الرئيسي للأغراض الصناعية والزراعية لمدينة السماوة، محافظة المثنى والتي تقع في الجزء الجنوبي الغربي من العراق. يتم وضع خط أنابيب الصرف الصحي في النهر، مما يؤثر بشكل مباشر على جودة المياه وبالتالي على الغطاء النباتي. تم إجراء دراسة معدنية مغناطيسية على الرواسب من أجل تحديد التلوث بالمعادن الثقيلة. حيث تم قياس الخصائص المغناطيسية في 250 عينة من الرواسب؛ تم قياس الحساسية المغناطيسية، والمغناطيسية المتبقية اللاهستيرية، والمغناطيسية المتبقية المتباينة الحرارة والتحليلات الحرارية المغناطيسية. تم إجراء تحليلات المعادن الثقيلة باستخدام المجهر الإلكتروني الماسح مع الأشعة السينية المنشطة للطاقة، كما تم إجراء تحليلات فلوروسنت الأشعة السينية لربط النتائج بالتعزيزات المغناطيسية. تظهر التحليلات الإحصائية أن متوسط قيم القابلية المغناطيسية كانت $3361.2 \times 10^{-8} \text{ م}^3\text{kg}^{-1}$ ، وكانت المغناطيسية المتبقية اللاهستيرية $628.9 \times 10^{-8} \text{ M}^3\text{kg}^{-1}$ ، كما تظهر التحليلات الحرارية المغناطيسية (العالية والمنخفضة) بوضوح المنحنيات النموذجية للمغناطيسية. تشير نتائج الخصائص المغناطيسية إلى أن المراحل المغناطيسية الرئيسية هي المغناطيسية أحادي المجال إلى متعدد المجالات (Multi-domain) الناجم عن مستجمعات (Single-domain) المياه المحيطة ومن الأنشطة البشرية. نتائج تحليلات المعادن الثقيلة (Heavy Metals) التي أجريت على عشر عينات مختارة تمت مقارنة نتائجها بالنتائج المغناطيسية. يُظهر الارتباط بين HM والحساسية المغناطيسية ارتباطاً إيجابياً بين الحساسية المغناطيسية وتراكيز العناصر Ca و Na و Mg و Fe و Pb و Cr.

تشير نتائج المعادن المغناطيسية إلى أنه يمكن استخدام معامل الحساسية المغناطيسية كمؤشر للمعادن الثقيلة.

معلومات الارشيف

تاريخ الاستلام: 27- اغسطس-2024

تاريخ المراجعة: 20- اكتوبر-2024

تاريخ القبول: 15- يناير- 2025

تاريخ النشر الإلكتروني: 01- يناير- 2026

الكلمات المفتاحية:

تلوث التربة،

المعدنية المغناطيسية،

العناصر الثقيلة،

المراسلة:

الاسم: نورس امين

Email: nawrass@mu.edu.iq

DOI: [10.33899/injes.v26i1.60182](https://doi.org/10.33899/injes.v26i1.60182), ©Authors, 2026, College of Science, University of Mosul.

This is an open-access article under the CC BY 4.0 license (<http://creativecommons.org/licenses/by/4.0/>).

Introduction

The river sediments are generated from bedrock weathering, organic matter, erosion, or anthropogenic activities (Perry and Taylor, 2007), which would be of great interest in carrying contaminants that reflect on humans. Anthropogenic activities, such as heavy metals, play a crucial role in polluting the environment, and they represent the majority of contaminants found in the river sediments caused by different sources such as irrigation, land use near the river, fuel combustion, industrial waste disposal, or agricultural waste (Sudarningsih et al., 2023).

Many researchers have reported monitoring heavy metals in soils and sediments using magnetic susceptibility techniques, where the magnetic susceptibility increases with increasing heavy metal concentrations. This method is considered efficient, fast, and cost-effective (Evans and Heller, 2003).

The accumulation of heavy metals has been evaluated in sediments from Sawa Lake in southern Iraq using magnetic mineralogy techniques. Selected heavy metal concentrations were measured and correlated with magnetic susceptibility concentrations. The results revealed an

insignificant correlation between magnetic susceptibility and heavy metals due to the low concentrations of magnetic signals in the lake sediments (Ameen et al., 2019).

In another study, the level of contamination in sediments from river streams collected from the Arc River (Provence, France) was assessed by rock-magnetic methods, to recognize magnetic particles produced by industrial to find a connection between magnetic pollution and heavy metal concentrations. The findings showed that human activity is the source of the magnetic variances identified in the riverbank sediments of the streams since these variances are positively correlated with Pb, Zn, Fe, and Cr concentrations (Desenfant et al., 2004).

The concentration of anthropogenic heavy metals found in both highly and slightly contaminated soil cores from a forest near a steel mill at Leoben, Austria, was measured by magnetic susceptibility analyses. In naturally contaminated soil, the magnetic susceptibility method proved to be an effective tool for semi-quantitatively defining the concentrations of heavy metals in soils. The results showed that there is a boundary depth that indicates the transition from the deeper “unpolluted” zone to the contaminated zone (Blaha et al., 2008).

This study aims to examine the magnetic signature of river sediments collected from the Euphrates River in Samawa City (Al Muthanna province) in southern Iraq, and to correlate the magnetic concentration with the heavy metals, given that heavy metal pollution could cause an increase in the magnetic concentration.

Materials and Methods

Geology and Geomorphology

The Euphrates River flows through the Mesopotamian Plain and ultimately merges with the Tigris River near the town of Al-Qurnah. The Mesopotamian Plain's sediments are mostly made of silt and clay (Sissakian and Al-Ansari, 2019). In the Mesopotamian Plain, small smooth and extremely flat depressions are frequent as morphological characteristics, having a few hundred square meters to several hundred square kilometers area, which cover different areas. The larger shallow depressions are found close to the area where the Abu Jir active fault zone links the western and southern deserts to the Mesopotamian plain; they are primarily sag depressions that show evidence of neotectonic activity (Sissakiana et al., 2021).

Study area location and sampling

The Study area is located in the Euphrates River, which crosses the city of Samawa, Al Muthanna province, with coordinates $31^{\circ}19'34.80''$ N, $45^{\circ}15'6.78''$ E. The type of sediments mainly consists of alluvial sediments (clay, silt) carried by rushing streams (Fig. 1).

Two hundred fifty sediment samples were collected from the bottom of the river using a shovel at intervals of one meter between the samples, and then stored in plastic bags and labeled.

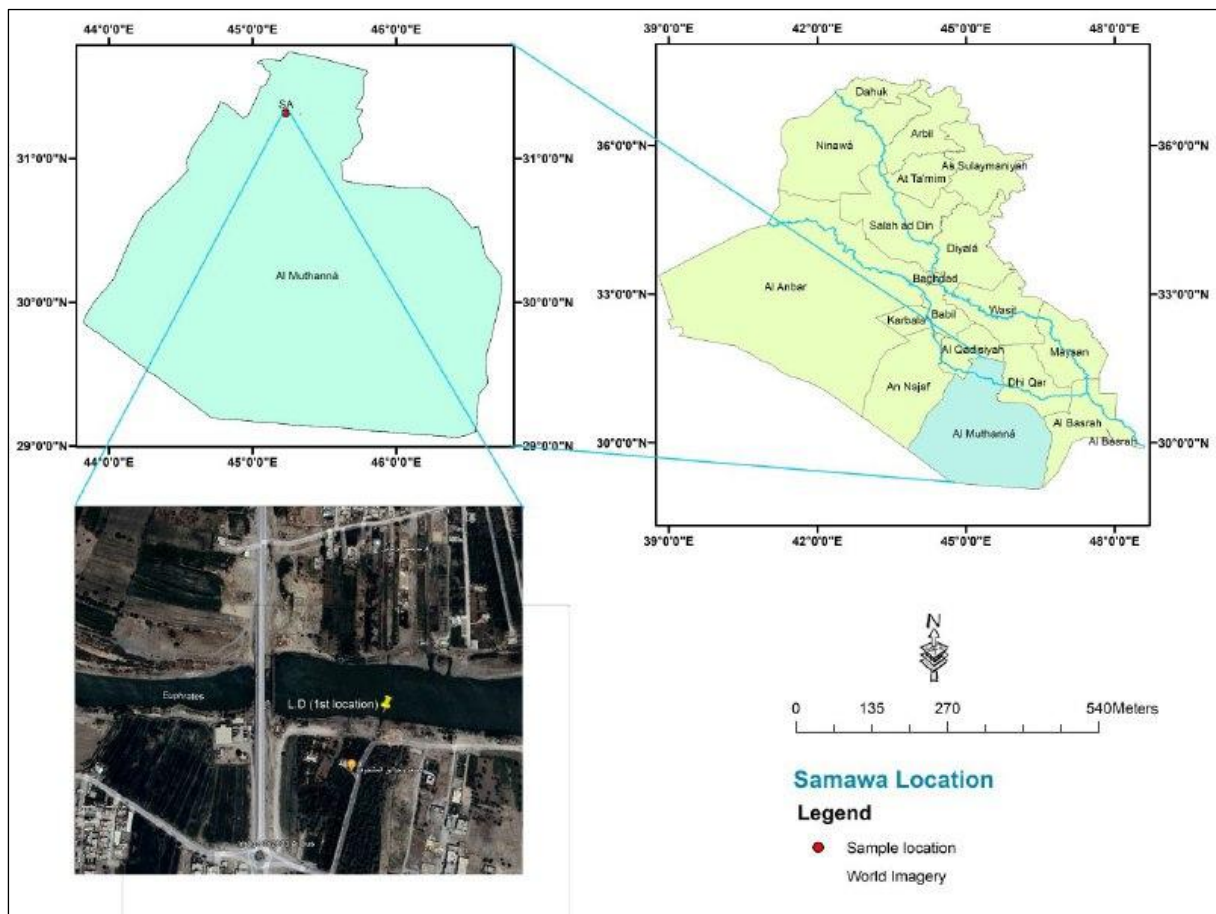


Fig. 1. Location maps of the study area

Laboratory Measurements

Magnetic measurements

The collected samples were transported to the Earth Magnetism Laboratory at the German Research Center for Geosciences (GFZ) located in Potsdam, Germany, in August 2023. Sample preparation has been performed, where the samples are air dried, sieved to remove the organic matter, and packed into small cubic plastic boxes 6 cm^3 , tightly closed to perform a series of magnetic measurements.

Magnetic susceptibility represents the concentrations of the ferrimagnetic minerals (such as iron-oxides, -hydroxides, and -sulphides), which expresses the dominance of magnetite. An AGICO Multi-function Kappabridge MFK1A was used to ascertain low-field susceptibility (κ_{LF}) (converted to mass-specific $\chi\text{ m}^3\text{kg}^{-1}$). Grain size distribution was estimated using several magnetic parameters, such as frequency-dependent susceptibility ($\kappa_{fd\%}$) (Hanesch and Petersen, 1999; Dearing et al., 1996a) measured at five frequencies (475, 825, 1525, 2675, 4775) Hz using AGICO MFK1 Kappabridge, to identify domain state via grain sizes (Jordanova and Jordanova, 1999). An eight-sample holder from 2G Enterprises' 755 SRM long-core magnetometer was used to perform anhysteretic remanent magnetization (ARM) and normalized AF demagnetization curves of ARM. The ARM was applied along the z-axis of the samples using a 100 mT AF field and a 0.05 mT static field. The ARM was then represented as the susceptibility of ARM (χ_{ARM}). A 2G Enterprises 660 pulse magnetizer was used to induce isothermal remanent magnetization (IRM), which was then measured using a Molyneux spinning magnetometer at two intensities, a backfield of 300 mT and 1000 mT, which is referred to as saturation isothermal remanent magnetization (SIRM). The S-ratio is calculated according to Bloemendal et al. (1992) equation, which is described as $\kappa_{fd\%} = [(\kappa_{LF} - \kappa_{HF}) / \kappa_{LF}] \times 100$. For pure hematite (Fe_2O_3), the S ratio is around 0; for both magnetite (Fe_3O_4) and

greigite (Fe_3S_4), it is around 1 (Rohrmüller et al., 2017). Using an AGICO Multi-function Kappabridge MFK1A, thermomagnetic analyses were carried out on bulk samples to measure low-field magnetic susceptibility versus temperature (κ -T curves) for determining the Curie temperature of magnetic minerals. Continuous measurements were performed from room temperature to 700 °C and back to room temperature using a Bartington furnace in free air (high temperature), and at low temperature using liquid nitrogen.

Heavy metal analyses

Scanning electron microscopy (SEM) and X-ray fluorescence (XRF) analyses were performed on selected samples to support the magnetic results. SEM was performed using a TESCAN MIRA3 SEM instrument. SEM can provide more details about fine grains and determine the mineralogy of the samples using SEM and energy dispersive X-ray (EDX) examinations to visualize the surface composition and shape of the extracted magnetic granules (Tamuntuan et al., 2015). XRF spectrometry was used to determine the concentration and source of the heavy metals in the study area (Oudeika et al., 2020). Concentrations (Al, Fe, Ca, Na, Si, Mg) of selected samples were measured. Heavy metal concentrations were measured using a Panalytical XRF System.

Results and Discussion

Magnetic Properties

Magnetic results are summarized in Table 1 and shown in Fig. 2. The Magnetic susceptibility of sediments is able to be employed for tracking pollutant sources. χ of sediment samples collected from the Euphrates River in Samawa City, Al Muthanna province, ranges at $2923.03 \times 10^{-8} \text{ m}^3\text{kg}^{-1}$ to $4039.29 \times 10^{-8} \text{ m}^3\text{kg}^{-1}$ with the mean value of $3361.23 \times 10^{-8} \text{ m}^3\text{kg}^{-1}$. ARM and SIRM have similar distribution patterns; χ , χ_{ARM} , and SIRM displayed a similar trend with the mean values of $3361.23 \times 10^{-8} \text{ m}^3\text{kg}^{-1}$, $628.98 \times 10^{-8} \text{ m}^3\text{kg}^{-1}$, and $2952.60 \text{ Am}^2\text{kg}^{-1}$, respectively, indicating that ferromagnetic minerals are dominant.

Table 1: Magnetic parameters of sediments from the Euphrates River.

Magnetic parameters	$\chi \times 10^{-8} [\text{m}^3/\text{kg}^{-1}]$	$\chi_{\text{ARM}} \times 10^{-8} [\text{m}^3\text{kg}^{-1}]$	SIRM [$\text{Am}^2\text{kg}^{-1}$]	$\kappa_{\text{fd}} [\%]$	S-ratio
Min.	2923.03	400.18	2390.90	0.35	0.96
Max.	4039.29	1354.12	5289.35	0.48	0.99
Mean	3361.23	628.98	2952.60	0.42	0.98
Median	3310.66	628.85	2918.06	0.42	0.98

The correlation between χ and χ_{ARM} , χ and SIRM is shown in Fig. 3. SIRM is more likely correlated with χ , with a correlation coefficient ($R^2 = 0.44$), while the correlation between χ_{ARM} and χ is less ($R^2 = 0.32$). The comparatively strong correlations show that ferrimagnetic minerals—such as magnetite and hematite—contribute more than paramagnetic minerals, such as biotite and pyrite (Sun et al., 1996).

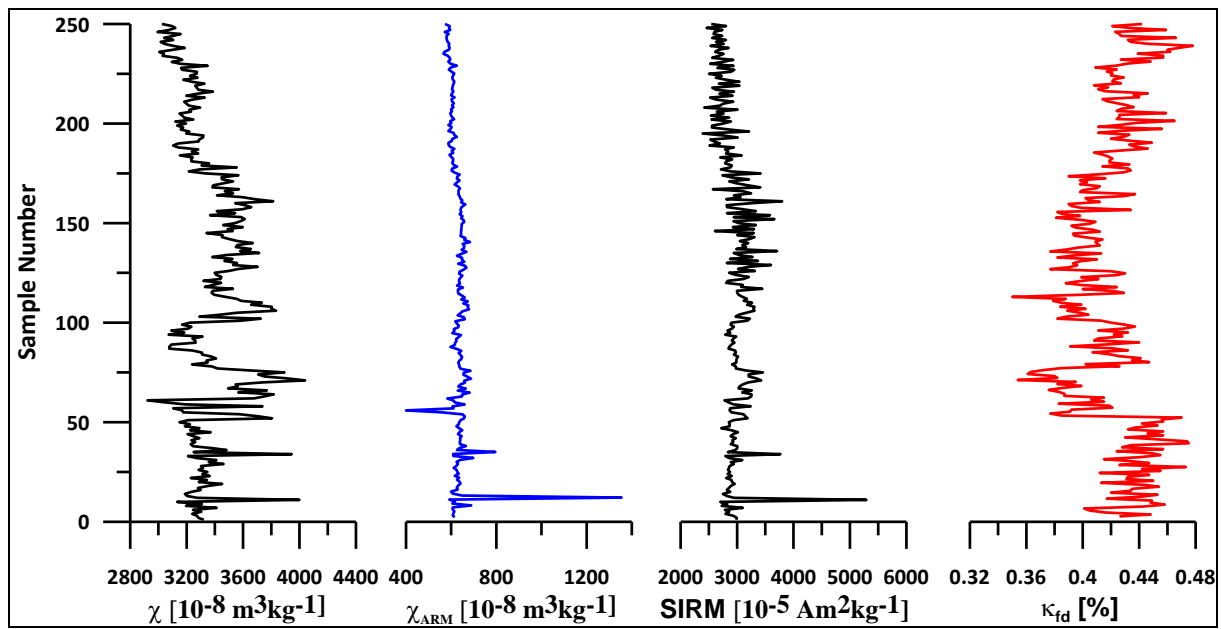


Fig. 2. Profiles of (A) mass-specific magnetic susceptibility; (B) anhysteretic susceptibility; (C) saturation isothermal remnant magnetization; (D) frequency-dependent susceptibility. All curves are versus the sample number.

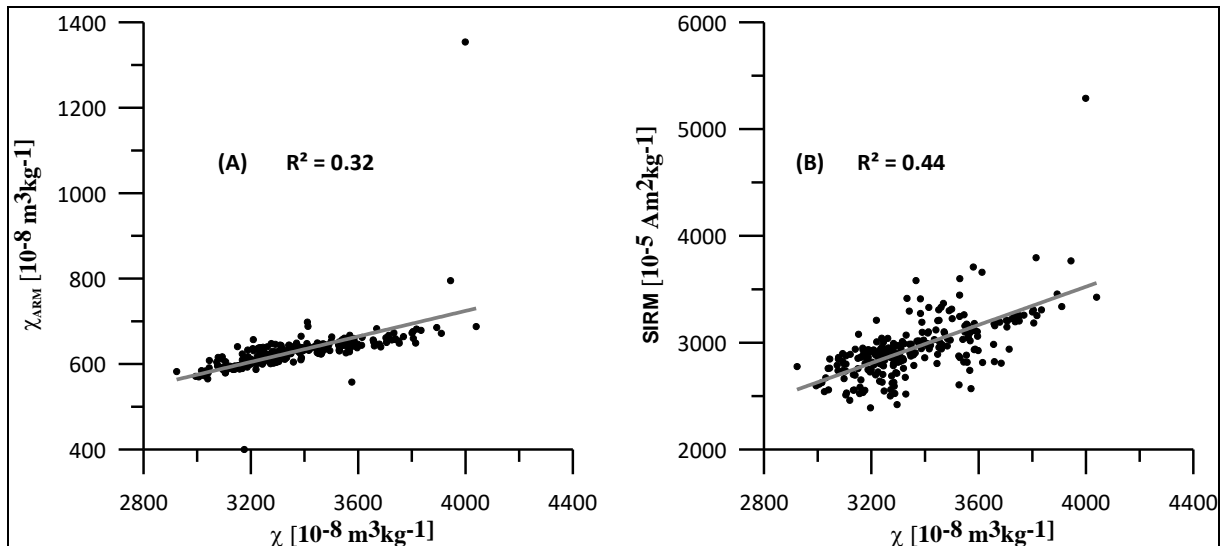


Fig. 3. Scatterplot of anhysteretic remnant magnetization and saturation isothermal remnant magnetization versus magnetic susceptibility.

Magnetic mineral grain size can be indicated by the values of χ_{ARM}/χ and SIRM/χ (Thompson and Oldfield, 1986; Evans and Heller, 2003). These ratios are frequently utilized in environmental magnetism for source identification and changes in grain size distribution as shown in Figure (4). The ratios of χ_{ARM}/χ and SIRM/χ drop as χ increases; in particular, the ratio χ_{ARM}/χ exhibits a dramatic decline with increasing grain sizes and clearly defined maximum values for carriers of magnetite/maghemitite in a single domain ($0.03 \mu\text{m}$). However, when magnetite grain sizes increase over $2 \mu\text{m}$ upwards, the ratio SIRM/χ progressively falls (Jordanova et al., 2014). S- ratio of sediments ranges from 0.96 to 0.99 with a mean value of 0.98 (Table 1), which indicates that soft magnetic minerals (magnetite) predominate in these samples (Shen et al., 2006). The percentage of frequency dependent susceptibility [$\kappa_{\text{fd}}\%$] ranges at 0.35% to 0.48 % with a mean value of 0.42% (Table 1). As stated in Dearing et al. (1996 b), the samples with $\kappa_{\text{fd}}\% < 6\%$ and $\chi_{\text{lf}} > 0.5 \times 10^{-6} \text{ m}^3 \text{kg}^{-1}$, the sediments are most likely polluted sediments with stable-single domain (SSD) and multi-domain (MD) ferrimagnetic grains.

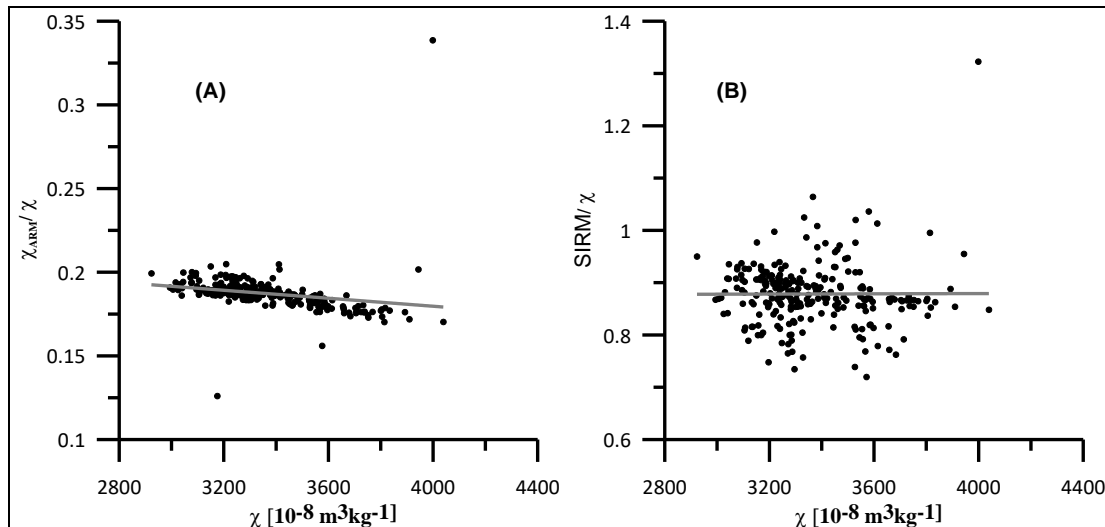


Fig. 4. Scatterplot of ratios χ_{ARM}/χ and SIRM/χ versus χ .

Temperature-dependent magnetic susceptibility measurements of selected sediment samples (κ -T) curves of low and high temperature are shown in Figure (5). Magnetic phases can be distinguished using high-temperature κ -T curves according to their Curie temperature or particularly the decomposition temperatures. High temperature-dependent magnetic susceptibility measurements can be used to identify the type of magnetic minerals based on their Curie temperature (Ju et al., 2004) as shown in Figure (5). During heating cycle, magnetic susceptibility would display a drop when reaching to 580 °C, which represents the Curie temperature of magnetite, and reaching its baseline at around 580°C (Thompson and Oldfield, 1986) proving the presence of magnetite in the samples. According to Hu et al. (2008), heating could result in the formation of more magnetic minerals because the susceptibility increase during cooling cycle in comparison to heating cycle when the temperature lower than 500 °C. The low temperature-dependent susceptibility (blue curves in Fig. 5) is a noticeable shift in susceptibility seen in all samples around -150 °C, which obviously show 'Verway transition' indicating the existence of magnetite (King and Williams, 2000).

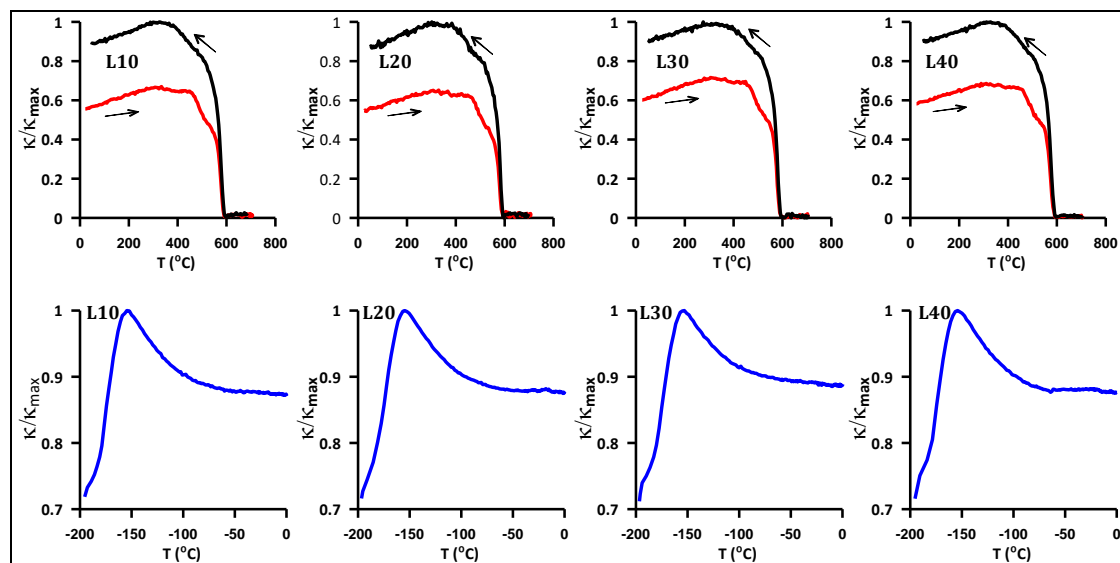


Fig. 5. Thermomagnetic analyses of selected sediment samples; the upper curves are for high temperature measurements; the red curve is for the heating cycle, and the black curve is for the cooling cycle; the lower curves are for low temperature measurements of the same samples.

Heavy metal (HM) analyses

Fig. 6 displays SEM pictures along with energy dispersive X-ray (EDX) analysis of particular samples. The X-ray indicates that the desired amount of Fe-minerals is present in Figure (6A, B), but seeing it in the image is difficult because of several issues. In contrast, Fig. 6C demonstrates the presence of a magnetic particle (spherical), indicating that the anthropogenic activities are the main source of the magnetic minerals.

Concentrations of Ca, Cr, Mg, Fe, Pb, and Na were measured using X-ray fluorescence (XRF). A correlation between χ and HM is shown in Fig. 7. χ exhibits a positive correlation with Ca, Cr, and Mg, with correlation coefficients of 0.3, 0.4, and 0.2, respectively, while the correlations of (Fe, Pb, and Na) are negative.

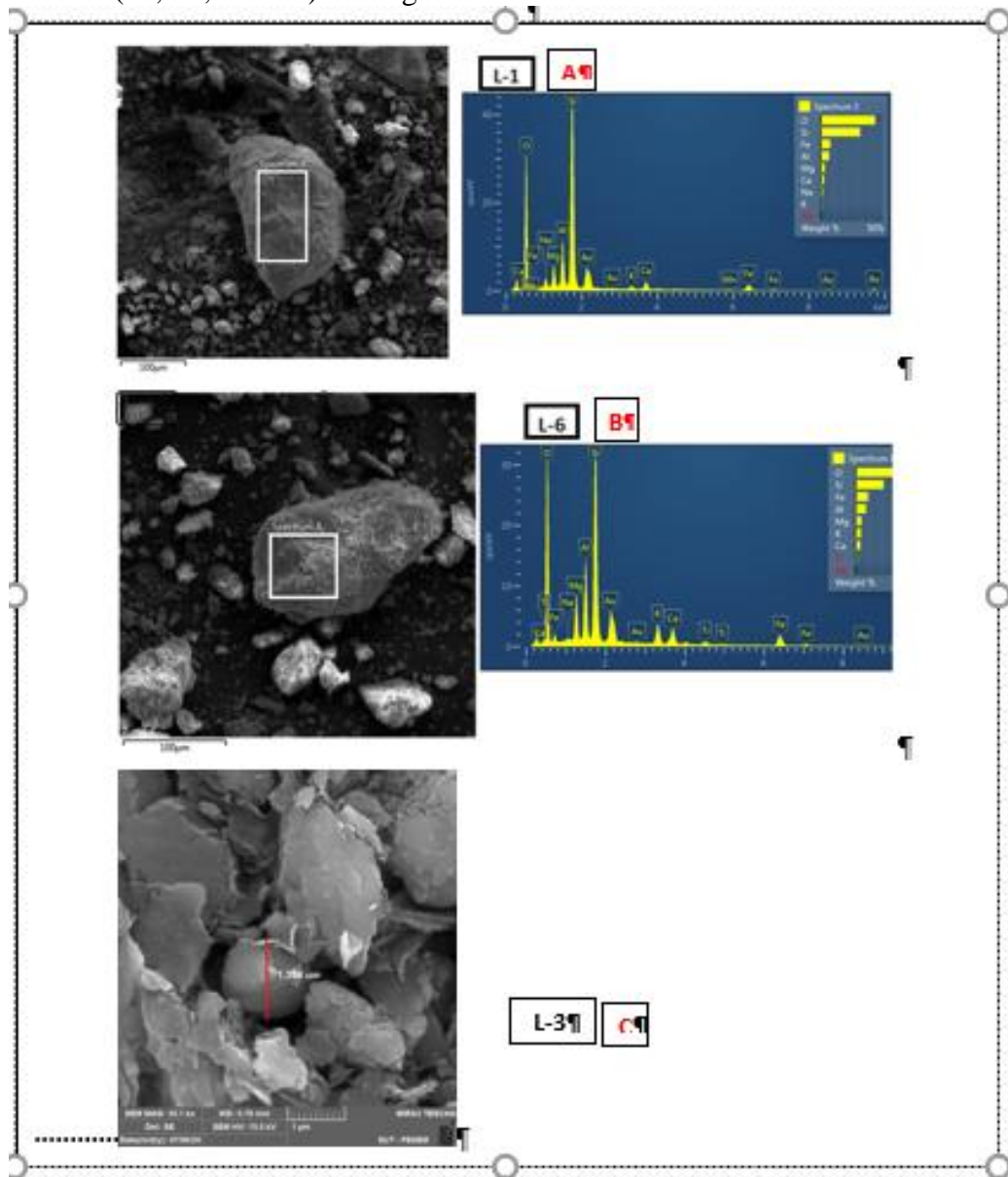


Fig. 6. Scanning Electron Microscopy images and energy dispersive X-ray analyses of selected samples: A (L1), B (L6), and C (L3) SEM micrographs showing a spherical magnetic particle of $\sim 1.35 \mu\text{m}$ diameter.

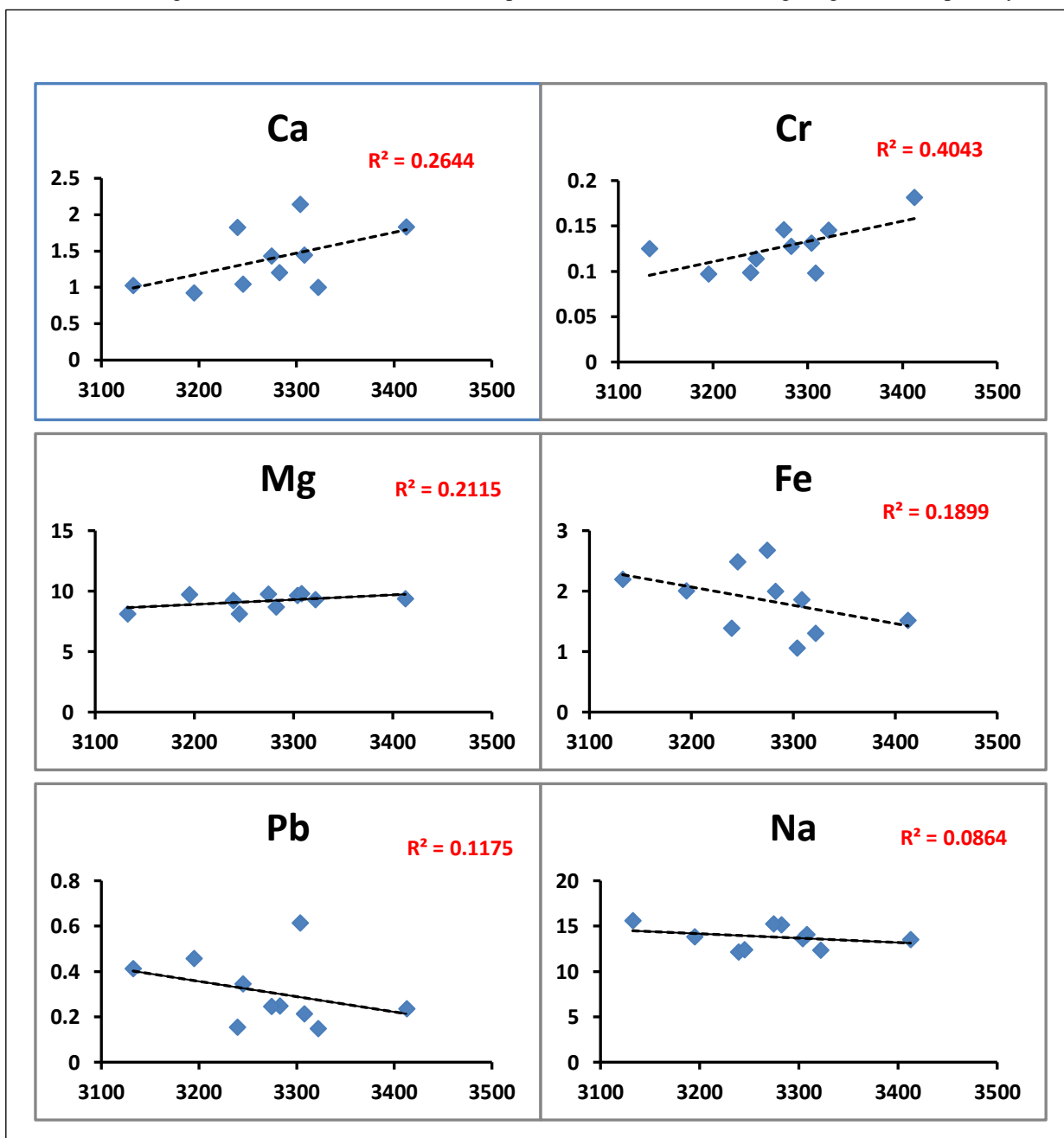


Fig. 7. Correlation of χ versus the heavy metals' concentrations of (Ca, Cr, Mg, Fe, Pb, and Na) in ppm of selected samples (L1-L10).

Conclusion

1. The concentration-dependent magnetic parameters (χ , χ_{ARM} , and SIRM) exhibit very high values. The correlation between these parameters suggests that ferrimagnetic minerals such as magnetite and hematite contribute significantly more than paramagnetic minerals.
2. As χ grows, the ratios of χ_{ARM}/χ and $SIRM/\chi$ decrease. In particular, the ratio χ_{ARM}/χ shows a sharp decline with larger grain sizes and has maximum values that are well-defined for single-domain magnetite/maghemitic carriers ($0.03 \mu\text{m}$). Furthermore, since the χ_{lf} is $> 0.5 \times 10^{-6} \text{ m}^3 \text{ kg}^{-1}$ and the $\kappa_{fd}\% < 6\%$. Dearing et al. (1996 b) stated that the sediments are most likely polluted with stable single-domain (SSD) and multi-domain (MD) ferrimagnetic grains.
3. Thermomagnetic measurements are of low temperature-dependent susceptibility for all samples, suggesting that susceptibility appears to transfer close to -150°C , clearly showing

the 'Verway transition', and indicating the existence of magnetite. High temperature is clearly shown to demonstrate the Curie temperature of magnetite (580 °C).

4. Energy dispersive X-ray (EDX) and SEM studies of a subset of samples show the existence of a spherical magnetic particle, which suggests the effects of anthropogenic activities, and the appropriate concentration of ferrimagnetic minerals in the samples.
5. Correlation between χ and XRF analyses shows a positive correlation of χ with (Ca, Cr, and Mg), while a negative correlation between χ and (Fe, Pb, and Na).

Acknowledgements

The author would like to express gratitude to Dr. Norbert Nowaczyk from Helmholtz Centre Potsdam (GFZ), German Centre for Geoscience, Germany, for granting free entry to the magnetic laboratory and providing all the new techniques used for measurements.

Conflict of Interest

The author declares that there are no conflicts of interest regarding the publication of this manuscript.

References

Ameen, N., Rasheed, L. and Khwedim, K., 2019. Evaluation of Heavy Metal Accumulation in Sawa Lake Sediments, Southern Iraq Using Magnetic Study. *Iraqi Journal of Science*, Vol. 60, No. 4, pp. 781-791. <http://doi.org/10.24996/ijjs.2019.60.4.12>.

Blaha, U., Appel, E. and Stanjek, H., 2008. Determination of Anthropogenic Boundary Depth in Industrially Polluted Soil and Semi-Quantification of Heavy Metal Loads Using Magnetic Susceptibility, *Environmental pollution*, Vol. 156, pp. 278–289, <https://doi.org/10.1016/j.envpol.2008.02.013>.

Bloemendaal, J., King, J.W., Hall, F.R. and Doh, S.J., 1992. Rock Magnetism of Late Neogene and Pleistocene Deep-Sea Sediments: Relations to Sediment Source, Digenetic Process, and Sediment Lithology. *Journal of Geophysical Research*, Vol. 97, pp. 4361-4375. <https://doi.org/10.1029/91JB03068>.

Dearing, J.A., Dann, R.J.L., Hay, K., Lees, J.A., Loveland, P.J., Maher, B.A. and O'Grady, K., 1996a. Frequency-Dependent Susceptibility Measurements of Environmental Materials. *Geophysical Journal International*, Vol. 124, pp. 228–240. <https://doi.org/10.1111/j.1365-246X.1996.tb06366.x>.

Dearing, J.A., Hay, K.L., Baban, S.M.J., Huddleston, A.S., Wellington, E.M.H. and Loveland, P.J. 1996b. Magnetic Susceptibility of Soil: an Evaluation of Conflicting Theories Using a National Data Set. *Geophysical Journal International*, Vol. 127, pp. 728–734, 1996. <https://doi.org/10.1111/j.1365-246X.1996.tb04051.x>.

Desenfant, F., Petrovský, E. and Rochette, P., 2004. Magnetic Signature of Industrial Pollution of Stream Sediments and Correlation with Heavy Metals: Case Study from South France. *Water, Air, and Soil Pollution*, Vol. 152, pp. 297–312. <https://doi.org/10.1023/B:WATE.000015356.88243.f>.

Evans, M.E. and Heller, F., 2003. Environmental Magnetism: Principles and Applications of Enviromagnetics, in: *International Geophysics Series*, Vol. 86, Academic Press, Amsterdam. <https://doi.org/10.1144/1470-9236/04-103>

Hanesch, M. and Petersen, N., 1999. Magnetic Properties of a Recent Parabrown-Earth from Southern Germany. *Earth Planet. Science Letters*, Vol. 169, pp. 85–97. <https://doi.org/10.1016/S0012-821X%2899%2900076-X>

Assessing the Environmental Situation of Euphrates River Sediments Using Magnetic Susceptibility.....

Hu, S.Y., Duan, X.M., Shen, M.J., Blaha, U., Roesler, W., Yan, H.T., Appel, E., Hoffmann, V., 2008. Magnetic Response to Atmospheric Heavy Metal Pollution Recorded by Dust-Loaded Leaves in Shougang Industrial Area, Western Beijing. *Chinese Science Bulletin*, Vol. 53, No. 10, pp. 1555–1564. <https://doi.org/10.1007/s11434-008-0140-9>

Jordanova, D. and Jordanova, N., 1999. Magnetic Characteristics of Different Soil Types from Bulgaria. *Studia Geophysica Et Geodaetica*, Vol. 43, pp. 303–318. <https://doi.org/10.1023/A:1023398728538>.

Jordanova, D., Jordanova, N. and Petrov, P., 2014. Magnetic Susceptibility of Road Deposited Sediments at a National Scale – Relation to Population Size and Urban Pollution. *Environmental Pollution*, Vol. 189, pp. 239–251. <https://doi.org/10.1016/j.envpol.2014.02.030>.

Ju, Y.T., Wang, S.H., Zhang, Q., Wang, L.D., Deng, C.L., 2004. Mineral Magnetic Properties of Polluted Topsoils: a Case Study in Sanming City, Fujian Province, Southeast China. *Chinese Journal of Geophysics*, Vol. 47, No. 2, pp. 282–288. (in Chinese). http://www.geophy.cn/en/article/id/cjg_63?viewType=HTML

King, J.G. and Williams, W., 2000. Low-Temperature Magnetic Properties of Magnetite. *Journal of Geophysical Research*, Vol. 105, No. B7, pp. 16427–16436. <https://doi.org/10.1029/2000JB900006>.

Oudeika, M.S., Altinoglu, F.F., Akbay, F. and Aydin, A. 2020. The Use of Magnetic Susceptibility and Chemical Analysis Data for Characterizing Heavy Metal Contamination of Topsoil in Denizli City, Turkey. *Journal of Applied Geophysics*, Vol. 183, pp. 104208. <https://doi.org/10.1016/j.jappgeo.2020.104208>.

Perry, C. and Taylor, K., 2007. *Environmental Sedimentology*, Blackwell Publishing, Oxford. <https://www.wiley.com/en-us/Environmental+Sedimentology-p-9781444309003>

Rohrmüller, J., Kämpf, H., Geiß, E., Großmann, J., Grun, I., Mingram, J., Mrlna, J., Plessen, B., Stebich, M., Veress, C., Wendt, A. and Nowaczyk, N. 2017. Reconnaissance Study of an Inferred Quaternary Maar Structure in the Western Part of the Bohemian Massif Near Neualbenreuth, NE-Bavaria (Germany). *International Journal of Earth Sciences*. <https://doi.org/10.1007/s00531-017-1543-0>

Shen, M., Hu, S., Blaha, U., Yan, H.T. and Hoffmann, V., 2006. A Magnetic Study of a Polluted Soil Profile at the Shijingshan Industrial Area, Western Beijing, China. *Chinese Journal of Geophysics*, Vol. 49, No. 6, pp. 1665–1673. (in Chinese). <https://doi.org/10.1002/cjg2.980>

Sissakian, V.K. and Al-Ansari, N., 2019. Geography, Geomorphology, Stratigraphy and Tectonics of the Euphrates River Basin. *Journal of Earth Sciences and Geotechnical Engineering*, Vol. 9, No. 4, pp. 315–337.

Sissakiana, V.K., Al-Ansari, N. and Adamoc, N., 2021. Geomorphology, Stratigraphy and Tectonics of the Mesopotamian Plain, Iraq: A Critical Review. *Geotectonics*, 2021, Vol. 55, No. 1, pp. 135–160.

Sudarningsih, S., Pratama, A., Bijaksana, S., Fahruddin, F., Zanuddin, A., Salim, A., Abdillah, H., Rusnadi M. and Mariyanto, M., 2023. Magnetic Susceptibility and Heavy Metal Contents in Sediments of Riam Kiwa, Riam Kanan and Martapura Rivers, Kalimantan Selatan Province, Indonesia. *Heliyon*, Vol. 9, Issue 6, e16425. ISSN 2405-8440, <https://doi.org/10.1016/j.heliyon.2023.e16425>.

Sun, Z., Hu, S. and Ma, X., 1996. A Rock-Magnetic Study of Recent Lake Sediments and its Palaeoenvironmental Implication. *Acta Geophysica Sinica*, Vol. 39, No. 2, pp. 178–187. (in Chinese). http://www.geophy.cn/en/article/id/cjg_4077

Tamuntuan, G., Bijaksana, S., King, J., Russell, J., Fauzi, U., Maryunani, K., Aufa, N. and Safiuddin, L.O., 2015. Variation of Magnetic Properties in Sediments from Lake Towuti, Indonesia, and its Paleoclimatic Significance. *Palaeogeography, Palaeoclimatology, Palaeoecology*, Vol. 420, pp. 163-172. <https://doi.org/10.1016/j.palaeo.2014.12.008>.

Thompson, R. and Oldfield, F., 1986. Environmental Magnetism. London: Allen and Unwin, Winchester, Mass., pp. 1–227. <https://doi.org/10.1007/978-94-011-8036-8>